MODELING SHARAD ECHOES FROM HIRISE-DERIVED STRATIGRAPHY OF THE NORTHERN POLAR LAYERED DEPOSITS OF MARS. D. C. Nunes[1], S. Christian[2], J. W. Holt[2], S. E. Smrekar[1], and R. J. Phillips[3], [1]Jet Propulsion Laboratory, California Institute of Technology, Pasadena CA 91109 (Daniel.Nunes@jpl.nasa.gov), [2]Jackson School of Geosciences, University of Texas, Austin TX 78758, [3]Southwest Research Institute, Boulder CO 80302

Introduction: Since the early days of Mariner 9, the Martian polar layered deposits (PLD) were suspected to be large volatile repositories [1]. Alternating bright and dark layers exposed at the walls of spiral troughs incising the PLD, and also at their at marginal scarps, suggested variations in the proportion of silicate impurities in the ice resulting from oscillations in the depositional regime [1,2,3,4]. Variations in insolation arising from obliquity and orbital eccentricity cycles was an early and continues to be the most accepted model for driving the variations in depositional regime and the PLD layering [4,5].

Much work has gone into characterizing and mapping the geomorphology and composition of the PLD as seen from their surface, and into modeling the formation and stability of the PLD. But it was not until the arrival of MARSIS (Mars Advanced Radar for Subsurface and Ionospheric Sounding [6]) and SHARAD (Shallow Radar [7]) at Mars that direct investigation of the PLD interior was possible. Signal from both sounders have penetrated to the base of the PLD and yielded a bulk permittivity of ~3 for the deposits; this is consistent with a composition of nearly pure water ice [8,9]. SHARAD, because of its higher vertical resolution, is better suited to map the layered structure of the PLD [10]. In fact, analysis of SHARAD data has focused on mapping the internal layers, which is slowly revealing the internal structure and sedimentary history of the deposits [e.g. 11,12].

Here we instead concentrate on how layer thickness and composition affect the interaction of SHARAD signals in producing observable echoes.

Previous Work: In preparation for the arrival of the Mars Reconnaissance Orbiter (MRO) at Mars, *Nunes and Phillips* (2006) [NP06, 13] conducted a predictive modeling exercise to characterize the response of the PLD to the SHARAD signal. Stratigraphy in their model consisted of a vertical albedo profile derived from MOC, THEMIS, and MOLA data of the layered exposure in one of the North PLD (NPLD) troughs. This profile not only provided the thicknesses of the different layers, but also served as a basis to their respective compositions through the assumption that variations in albedo result from differences in dust content in the ice. To finally convert profile composition into permittivity, to which the radar signals are sensitive, NP06 applied the variations in dust and ice content into mixing formulae [e.g. 14]. A major source of uncertainty in the permittivity profiles so obtained is our ignorance of the permittivity of the silicate component of the mixture. For example, bulk permittivity of basalts varies between 4.9 and 9.8 [14]. In contrast, the permittivity of water ice for martian temperatures and SHARAD frequencies resides at ~ 3.10 ± 0.05 [13]. Finally, the propagation of the SHARAD chirp (20 MHz center frequency, 10 MHz bandwidth, and 85 µs width) through the permittivity profiles in NP06 followed the model of [15] for normal incidence of plane waves onto layered media.

NP06 successfully predicted SHARAD observations in that the fine layering seen in the PLD would produce observable reflections even in the case of a low dust content in the layers (which appears to be the case based on the ~3 bulk permittivity of the PLD). This abstract represents the first step in closely comparing the NP06 model to the actual radargram data obtained by SHARAD and deriving compositional constrains.

Model Input: In this work we extract albedo and relief information from HiRISE data in order to produce the dielectric profile in the same fashion as NP06.

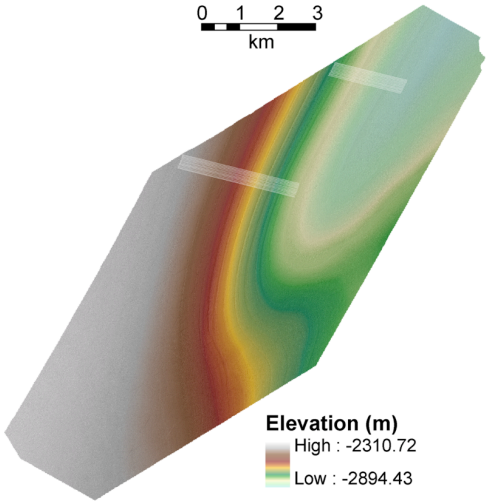

Fig. 1 – DTEPC_001738_2670_001871_2670_U01 HiRISE DEM of a NPLD trough [16], centered approximately at 87.09ºN, 92.70ºE. Color denoting elevation is superposed onto shaded-relief (right illumination). The couple of light-toned rectangles on the DEM correspond to groups of profiles acquired for this study.

Overlapping HiRISE frames PSP_001738_2670 and PSP_001871_2670 (87.09°N, 92.70°E) were used by the HiRISE team to produce a digital elevation model

(DEM) – Fig. 1. Multiple profiles allows us to investigate the effect of slope and roughness on the albedo of distinct marker beds. *Fishbaugh et al.* (2010) [16] analyzed this set of images and the accompanying DEM and determined a separation of 24 to 36 m between marker layers, this result being similar to the frequency analysis of *Milkovich and Head* (2005) [17]. However, the link between orbital cycles and the stratigraphy is complex and not yet resolved [16].

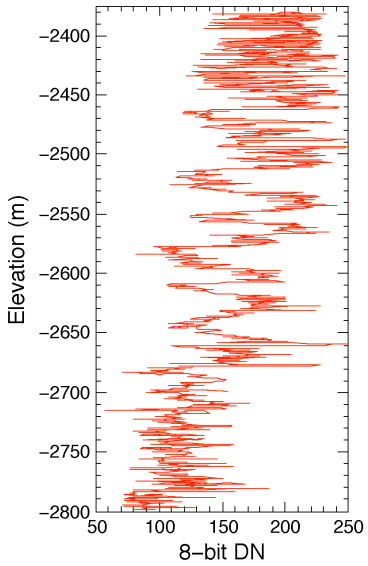

Fig. 2 – Brightness profile with respect to depth extracted from HiRISE DEM in Fig. 1.

SHARAD Data: To serve as a comparison for the models, we have extracted frames from multiple SHARAD (focused) radargrams crisscrossing the area of the HiRISE DEM in Fig. 1. Centered at 87.1639ºN, 97.8104ºE, a circle drawn to the surface isolated the frames of interest. The radius of the circle (R_s) was initially set at 1500 m, comparable to the cross-track resolution of SHARAD set by the 1st Fresnel zone [10]. Averaging of the selected frames, intended to reduce the incoherent noise, appears to mute the echoes from the subsurface layering. The layered signature stands out only when reducing R_s to < ~ 300 m.

Initial Results: Brightness profiles (such as that of Fig. 2) were resampled via cubic spline at regular depth interval (25 cm) in preparation for the propagation model. We scaled brightness values (8-bit digital number) to Lambertian albedo (A) via the approach of NP06, assigning a minimum dust fraction (ν) to the highest A, and maximum ν to the lowest A. Note that the scaling from brightness to A referred to radiometrically calibrated THEMIS data at a trough different from the one in Fig. 1; we will later conduct the conversion to A using collocated data sets. Note also that in order to prevent an artificial dielectric interface at the bottom, a layer composed of pure water ice lies beneath the layered section of the model to a depth of 2 km.

The simulations shown in Fig. 3 assume bright layers to be very clean (ν = 0.1%), while different cases are shown for maximum ν. As in NP06, reflections from individual layers merge to form broader peaks; this effect is more noticeable in cases where ν is higher (Fig.3). SHARAD data at smooth locations possess a noise floor of 40 dB. Assuming this to be the detection limit, and using a relatively high permittivity for the dust component, requires ν to exceed a few percent in the dark layers in order to produce detectable reflection (Fig. 3). More dust would be required if a lower dust permittivity is applied. Finally, for the PLD reflections above the noise floor, peak separation of ~0.4 μs appears to dominate the radargram. This corresponds to a separation of ~34 m, which is similar to one of the dominant wavelengths in the analyses of [16,17].

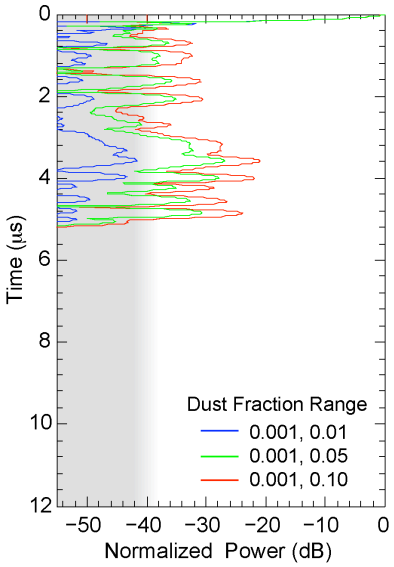

Fig. 3 – Simulated radargrams using the propagation model of NP06, the HiRISE brightness profile from Fig. 2, and different assumptions for dust loading. Shading corresponds to power below noise level. Permittivities of water ice and basaltic dust are, respectively, 3.15 + *i*6.3e-4 and 8.8 + *i*1.7e-2.

References: **[1]** Murray, B. C. et al. (1972) *Icarus*, *17*, 328-345. **[2]** Cutts J. A. (1973) *JGR*, *78*, 4231-4249. **[3]** Soderblom L. A. et al. (1973) *JGR*, *78*, 4197-4210. **[4]** Murray B. C. et al. (1973) *Science*, *180*, 638-640. **[5]** Laskar J. et al. (2002) *Nature*, *419*, 375-377. **[6]** Picardi G. D. et al. (2004) *PSS*, *52*, 149-156. **[7]** Seu R. et al. (2004) *PSS*, *52*, 157-166. **[8]** Picardi, G. et al. (2005) *Science*, *310*, 1925-1928. **[9]** Phillips R. J. et al.(2008) *Science*, *320*, 1182-1185. **[10]** Seu, R. et al. (2007) *JGR*, *112*, E05S05. **[11]** Milkovich S. M. et al. (2009) *JGR*, *114*, E03002. **[12]** Smith I. B. and J. W. Holt (2010) *Nature*, *465*, 450-453. **[13]** Nunes D. C. and R. J. Phillips (2006) *JGR*, *111*, E06S21. **[14]** Ulaby F. T. et al. (1986) *Microwave Remote Sensing*, Artech House, Norwood, MA. **[15]** Wait J. R. (1970) *Electromagnetic waves on stratified media*, Pergamon Press, New York, NY. **[16]** Fishbaugh K. E. et al. (2010) *GRL*, *37*, L07201. **[17]** Milkovich S. M. and J. W. Head (2005) *JGR*, *110*, E01005.